HEAT LOSSES FROM A FLUID FLOWING IN A BURIED PIPE

HAIM H. BAU

Department of Mechanical Engineering and Applied Mechanics, University of Pennsylvania, Philadelphia, PA 19104, U.S.A.

and

S. S. SADHAL

Department of Mechanical Engineering, University of Southern California, Los Angeles, CA 90007, U.S.A.

Abstract—Analytical solutions are presented for heat losses from a buried pipe. Two cases are considered. The first one involves a mixed (convective) boundary condition with a uniform heat transfer coefficient at the pipe surface which would be the case for turbulent flow. A simple approximate expression, accurate within 2%, is derived for the shape factor in this case. In the second case, a laminar flow with linear temperature variation along the pipe axis is considered. The coupling of the heat transfer process inside and outside the pipe requires simultaneous solution of the energy equations for these two regions. The complicated geometry is handled in an elegant manner with the use of the bicylindrical coordinate system. The results include the temperature distributions and the shape factor in each case.

NOMENCLATURE

a, scale factor for the bicylindrical coordinates (nondimensional), $\sinh \alpha_0$;
A_n, B_n, numerical coefficients;
Bi, Biot number $(hR)/k_2$;
D, location of the pipe axis beneath the surface [m];
e, unit vector in the pipe axis (z) direction;
g, metric coefficient, equation (8);
h, heat transfer coefficient [W m^{-2} K^{-1}];
k, thermal conductivity [W m^{-1} K^{-1}];
K, a constant, equation (23);
n, N, integers;
Nu, Nusselt number, $(hR)/k_1$;
Q, heat flow rate per unit length of the pipe;
r, radial coordinate, Fig. 1;
R, pipe radius [m];
S, shape factor, equation (19);
T, temperature [K];
u, velocity [m s^{-1}];
x, y, rectangular coordinates, Fig. 1;
z, coordinate along the pipe axis.

Greek symbols
α, β, bicylindrical coordinates, Fig. 1;
θ, temperature, equation (23) [K];
κ, thermal diffusivity [m^2 s^{-1}].

Superscripts
*, dimensional quantities;
$^-$, average.

Subscripts
1, values inside the pipe;
2, values outside the pipe;
b, bulk.

1. INTRODUCTION

IN RECENT years the problem of heat loss from a buried pipeline has received considerable attention. This problem arises, for example, in connection with oil lines, powerplant steam and water distribution lines, underground electrical powerline transmission, and in certain types of heat exchangers.

Approximate and exact steady state heat loss calculations are available in the literature for pipes with idealized boundary conditions such as isothermal surfaces [1–4] or uniform heat flux surfaces [5]. The approximate solutions are based on the superposition of infinite line heat source and sink solutions [1–3]. The exact solutions are obtained by the use of the bicylindrical coordinates [4, 5]. Some approximate time-dependent solutions are given by Ioffe [6] and by Martin and Sadhal [7].

All the above analyses refer to idealized scenarios (pipes with isothermal surfaces or uniform heat flux surfaces), which do not occur often in practice. The purpose of this paper is to consider a somewhat more realistic situation in which the thermal interaction between the fluid flowing in the pipe and the solid medium in which the pipe is buried is taken into consideration. Two cases are treated. First (section 3), we assume a mixed (convective) boundary condition with a uniform heat transfer coefficient at the pipe surface. Such a model is quite realistic when the fluid in the pipe is well mixed, as occurs in turbulent flow. In the second case (section 4), we assume fully developed laminar flow in the pipe. The temperature distri-

butions inside and outside the pipe are calculated simultaneously. For the sake of brevity, we shall refer to these two cases as turbulent and laminar, respectively. Finally, in section 5 we compare the laminar and turbulent cases. The results include the temperature distribution inside (for the laminar case only) and outside the pipe and the thermal resistance between the fluid and the medium surfaces as a function of the burial depth and the properties of the fluid and the solid medium.

2. FORMULATION

Consider a pipe of radius R buried at depth D below an isothermal (T_0) surface of a semi-infinite solid (Fig. 1). Fluid with bulk temperature T_b is flowing in the pipe.

In the first case, that of a turbulent flow in the pipe, we have to solve the heat equation for the solid medium

$$\nabla^2 T_2^* = 0 \tag{1}$$

with boundary conditions

$$T_2^* = T_0 \text{ at the medium surface}$$

and

$$-k_2 \frac{\partial T_2^*}{\partial r^*} = h(T_b - T_2^*) \quad \text{at } r^* = R \tag{2}$$

where T_i is the temperature distribution, k is the thermal conductivity, h is the heat transfer coefficient, and r^* is the radial coordinate (Fig. 1). Indexes 1 and 2 refer to conditions inside and outside the pipe, respectively. Asterisks denote dimensional variables which will later be made nondimensional.

For the case of laminar flow, we solve, in addition to equation (1), the energy equation for fully developed forced convection in the pipe

$$\left(\frac{1}{\kappa_1}\right)\mathbf{u} \cdot \nabla T_1^* = \nabla^2 T_1^* \tag{3}$$

where

$$\mathbf{u} = 2\bar{u}[1 - (r^*/R)^2]\mathbf{e}_z \tag{4}$$

is the axial velocity in direction z, $\mathbf{e}_z$ is the unit vector in

FIG. 1. The geometry of the problem and the bicylindrical coordinate system.

the z direction, κ_1 is the thermal diffusivity of the fluid, and $\bar{u}$ is the average velocity. We now have to satisfy at the pipe surface the conditions

$$T_1^* = T_2^* \tag{5}$$

and

$$k_1 \frac{\partial T_1^*}{\partial r^*} = k_2 \frac{\partial T_2^*}{\partial r^*} \quad \text{at } r^* = R.$$

We introduce nondimensional variables by scaling the length with R and the temperature with $(T_b - T_0)$. That is, we nondimensionalize the temperature as follows:

$$T_i = (T_i^* - T_0)/(T_b - T_0).$$

It is convenient to carry out the analyses by using the bicylindrical coordinate system (α, β, z) [3, 4]. This coordinate system is sketched in Fig. 1 and has the advantage that the boundary conditions are located along the coordinates. The coordinates $\alpha = 0$ and $\alpha = \alpha_0$ represent the medium and the pipe surfaces, respectively.

The transformation into bicylindrical coordinates is achieved by using the formula

$$x + iy = a \tanh\left(\frac{\alpha + i\beta}{2}\right), \tag{6}$$

$$0 < \alpha < \infty, \quad -\pi < \beta < \pi.$$

The Laplace operator takes the form

$$\nabla^2 = \frac{1}{g(\alpha, \beta)}\left(\frac{\partial^2}{\partial \alpha^2} + \frac{\partial^2}{\partial \beta^2}\right) \tag{7}$$

where

$$g(\alpha, \beta) = a^2(\cosh \alpha + \cos \beta)^{-2}. \tag{8}$$

The pipe surface (α_0) is described by the circle

$$(x - a\coth \alpha_0)^2 + y^2 = \frac{a^2}{\sinh^2 \alpha_0} \tag{9}$$

where

$$a = \sinh \alpha_0 \text{ and } a\coth \alpha_0 = D/R.$$

3. TURBULENT FLOW

In this section we assume that the heat transfer coefficient at the pipe surface is uniform. Such a situation may arise when the fluid in the pipe is well mixed as in turbulent flow. The equations (1) and (2), when rewritten in bicylindrical coordinates, have the form

$$\frac{\partial^2 T_2}{\partial \alpha^2} + \frac{\partial^2 T_2}{\partial \beta^2} = 0, \tag{a}$$

$$(\cosh \alpha_0 + \cos \beta)\frac{\partial T_2}{\partial \alpha} = Bi\, a(1 - T_2) \text{ at } \alpha = \alpha_0 \text{ (b)} \tag{10}$$

$$T_2(0, \beta) = 0 \tag{c}$$

where $Bi = \dfrac{hR}{k_2}$ is the Biot number.

The solution to equation (10a) with boundary condition (10c) is readily obtained in the form

$$T_2 = A_0 \alpha + \sum_{n=1}^{'} A_n \sinh n\alpha \cos n\beta. \qquad (11)$$

The coefficients A_n are to be established with the aid of boundary condition (10b). The resulting relationship is

$$(\cosh \alpha_0 + \cos \beta)\left(A_0 + \sum_{n=1}^{'} n A_n \cosh n\alpha_0 \cos n\beta\right)$$

$$= aBi\left(1 - A_0\alpha_0 - \sum_{n=1}^{'} A_n \sinh n\alpha_0 \cos n\beta\right). \qquad (12)$$

The factor $(\cosh \alpha_0 + \cos \beta)$ above causes some trouble since we cannot equate the infinite series in equation (12) on a term-by-term basis. However, we can overcome this difficulty by using the trigonometric identity

$$\cos \beta \cos n\beta = \tfrac{1}{2}[\cos(n+1)\beta + \cos(n-1)\beta]$$

to obtain a set of linear algebraic equations

$$A_0\left(1 + \frac{a\alpha_0 Bi}{\cosh \alpha_0}\right) + \tfrac{1}{2}A_1 = \frac{a Bi}{\cosh \alpha_0}$$

$$A_0 + A_1(\cosh^2 \alpha_0 + a Bi \sinh \alpha_0) + A_2 \cosh 2\alpha_0 = 0$$

$$\left(\frac{n-1}{2}\right)A_{n-1}\cosh(n-1)\alpha_0 + A_n(n\cosh n \alpha_0 \cosh \alpha_0$$

$$+ a Bi \sinh n\alpha_0)$$

$$+ \left(\frac{n+1}{2}\right)A_{n+1}\cosh(n+1)\alpha_0 = 0 \quad \text{for } n \geqslant 2. \quad (13)$$

This set of equations cannot be solved since any N equations involve $N + 1$ unknowns. However, A_n is a decreasing sequence and can be truncated at some $n = N$. Should we set $A_{N+1} = 0$, the above equations (13) can be solved in a closed form for any N.

An alternative method of solution is to supplement the set of equations (13) with an additional equation. This equation states that the amount of heat conducted from a unit length of pipe surface

$$Q^* = k_2(T_b - T_0)\int_{-\pi}^{\pi}\left(\frac{\partial T_2}{\partial \alpha}\right)d\beta$$

$$= A_0 2\pi k_2(T_b - T_0), \qquad (14)$$

is equal to the amount of heat lost by the fluid,

$$Q^* = ha(T_b - T_0)$$

$$\times \int_{-\pi}^{\pi}[1 - T_2(\alpha_0, \beta)]\frac{d\beta}{\cosh \alpha_0 + \cos \beta}. \qquad (15)$$

By equating equations (14) and (15) we obtain the supplementary equation

$$A_0\left(\alpha_0 + \frac{1}{Bi}\right) + \sum_{n=1}^{'} A_n \sinh n\alpha_0 (-1)^n e^{-n\alpha_0} = 1. \qquad (16)$$

We can now truncate equations (13) for some $n = N$ and solve them simultaneously with equation (16).

Both procedures described above are easy to apply. The equations are essentially tridiagonal, therefore no matrix inversion is necessary. We apply a modified version of the Gauss–Jordan elimination technique, in which a special provision is added to diagonalize equation (16). The second procedure described above usually leads to a quicker convergence; however, it is more susceptible to round-off errors.

The number of terms needed to achieve a desired accuracy is inversely proportional to α_0. For example, to achieve precision up to 3 significant digits, about 30 terms are needed for $\alpha_0 = 0.1$ while 2 are sufficient for $\alpha_0 \geqslant 2$.

Next, we investigate the behavior of the solution for large and small values of α_0.

For large values of α_0, (a pipe buried deep below the surface), we maintain only the first term in equation (11). Consequently we obtain

$$T_2 \sim \frac{Bi \, \alpha}{1 + Bi \, \alpha_0}. \qquad (17)$$

For even larger values of α_0 and moderate values of Bi, equation (17) is identical to the case of an isothermal pipe.

For small values of α_0, an asymptotic solution for T can be obtained in the form of a power series in α_0. The two leading terms in such a series are

$$T \sim \frac{a Bi \, \alpha}{\cosh \alpha_0 + \cos \beta}\left(1 - \frac{a Bi \, \alpha_0}{\cosh \alpha_0 + \cos \beta}\right). \quad (18)$$

These asymptotic expressions may be used to calculate the temperature field for small and large α_0 without evaluating the coefficients A_n from equation (13). They may be also used for yet another purpose.

Although the method of solution described above leads to exact results it is not convenient for engineering purposes. One would rather have a closed form approximate expression. By solving $\partial^2 T/\partial \alpha^2 = 0$ with the appropriate boundary conditions, we obtain the following expression for the temperature field:

$$T \approx \frac{a Bi \, \alpha}{\cosh \alpha_0 + \cos \beta + aBi\alpha_0}. \qquad (19)$$

It is easy to see that at the limits of large and small α_0, expression (19) behaves like the asymptotic solutions (17) and (18), respectively. Consequently, we may expect equation (19) to be a reasonable approximation of the temperature field for all values of α_0. To illustrate that this is indeed the case, we show in Fig. 2 exact (solid lines) and approximate (dashed lines) temperature profiles on the pipe surface for various burial depths (α_0) and for $Bi = 1$. The ordinate is the temperature $T_2(\alpha_0, \beta)$, and the abscissa is the coor-

dinate β. Clearly, the approximation (19) resembles quite well the exact solution. The discrepancy between the approximate and exact results is always smaller than 15%.

Another matter of interest for engineering purposes is the shape factor (S) which is defined by the ratio

$$S = \frac{Q^*}{2\pi k_2(T_b - T_0)} \qquad (20)$$

where Q^* is the heat transfer per unit length of the pipe. In accordance with equation (14), the exact value for S is

$$S = A_0. \qquad (21)$$

The corresponding value for large α_0 is found from equation (17) to be

$$S \sim \frac{Bi}{(\alpha_0 Bi + 1)}. \qquad (21a)$$

For small values of α_0, S is obtained from equation (18) as

$$S \sim Bi(1 - Bi\,\alpha_0\coth\alpha_0),$$

and the approximation based on equation (19) is

$$S \simeq \frac{Bi}{(1 + Bi^2\,\alpha_0^2 + 2Bi\,\alpha_0\coth\alpha_0)^{1/2}}. \qquad (22)$$

As may have been expected, for large and small values of α_0, equation (22), approaches the corresponding asymptotic results. We also compare the exact equation (21), and approximate equation (22), values of S. The agreement is excellent. The deviation between the two results is always smaller than 2%, with the approximate result (22) being always slightly below the exact one, equation (21). This means that for any practical purpose expression (22) can be used to calculate the shape factor. This is a rather exciting result since expression (22) is relatively simple and easy to apply compared to the exact expression. Yovanovich [8] has pointed out to us that expression (22) is
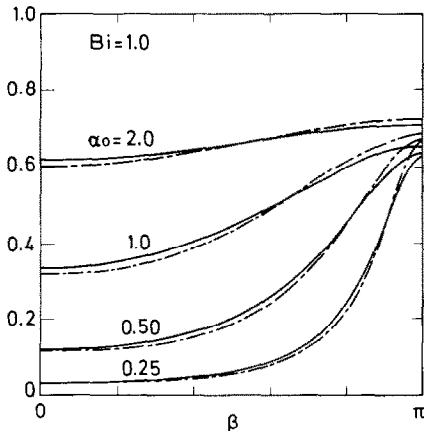

FIG. 2. Temperature distribution on the pipe surface for various burial depths and for $Bi = 1$. $\alpha_0 = 0.25, 0.5, 1$ and 2, correspond to $D/R = 1.031, 1.128, 1.543,$ and $3.762,$ respectively.
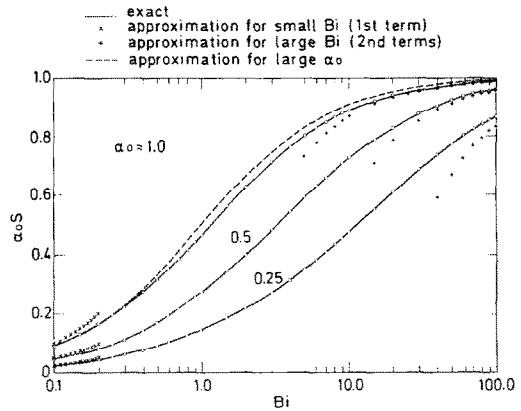

FIG. 3. The shape factor (S) is shown as a function of the Biot number (Bi) for various burial depths $\alpha_0 = 0.25, 0.5,$ and 1. ($D/R = 1.031, 1.128$ and 3.762). The solid lines and the circles represent the exact and approximate solutions respectively. The dashed curve, the $\times$ and the $+$ designate the approximate behavior for large α_0, small Bi and large Bi respectively.

actually a lower bound of (21). This matter is discussed in the Appendix. Figure 3 shows the shape factor as a function of the Biot number (Bi) for various burial depths (α_0). The abscissa is the Biot number, and the ordinate is the actual shape factor divided by the shape factor of an isothermal pipe $(1/\alpha_0)$. The solid lines represent the exact results from (21). The approximate calculation (22) is presented by circles in Fig. 3. Since the approximation (22) is so close to the exact solution, the circles and the solid lines actually coincide. The dashed line shows the approximation for large α_0, equation (21a), evaluated for $\alpha_0 = 1$. As α_0 increases, the difference between equation (21a) and (22) decreases. For $\alpha_0 \geqslant 2$, expression (21a) can be used with an error smaller than 1%. For small values of Bi, S behaves like Bi. This is shown in Fig. 3, using the notation $\times$. For large values of Bi, S behaves like

$$S \simeq \frac{1}{\alpha_0}\left[1 - \left(\frac{1}{Bi}\right)\left(\frac{\coth\alpha_0}{\alpha_0}\right)\right];$$

and as $Bi \to \infty$, $S \to (1/\alpha_0)$, which is the shape factor for an isothermal pipe. The behavior at large Bi values is denoted by the symbol $+$ in Fig. 3.

4. LAMINAR FLOW

In the previous section, we solved the heat transfer problem for the case of a uniform heat transfer coefficient on the pipe surface. One cannot assume, however, such uniformity in the case of laminar flow. In this case, the temperature profile is asymmetric with respect to the pipe axis. Consequently, the heat transfer coefficient is expected to have angular dependence. It is thus necessary to solve simultaneously for the temperature distribution inside and outside the pipe.

The equations which must be solved are (1), (3) and (5). In order to separate the variables in equation (3), we assume that the temperatures, T_1^* and T_2^*, vary linearly along the pipe axis. As a result we have

$$T_i^* = -\left(\frac{K\kappa_1}{2\bar{u}}\right)z + \theta_i(\alpha, \beta) \qquad (23)$$

where $K\kappa_1/2\bar{u} = $ constant, and indexes 1 and 2 refer to conditions inside and outside the pipe, respectively. The equations (1), (3) and (5) have the form

$$\nabla^2\theta_1 = -K[1 - (r/R)^2], \qquad (24)$$

$$\nabla^2\theta_2 = 0 \qquad (25)$$

with the boundary conditions

$$\theta_2(0, \beta) = 0 \qquad (26)$$

at the medium surface,

$$\theta_1(\alpha_0, \beta) = \theta_2(\alpha_0, \beta), \qquad (27)$$

$$k_1 \frac{\partial\theta_1(\alpha_0, \beta)}{\partial\alpha} = k_2 \frac{\partial\theta_2(\alpha_0, \beta)}{\partial\alpha} \qquad (28)$$

at the pipe surface (α_0), and

$$\theta_1(\alpha, \beta) < \infty \quad \text{as } \alpha \to \infty. \qquad (29)$$

To obtain a solution for equation (24), we first obtain an axially symmetrical particular solution and add to it a solution of the homogeneous equation $\nabla^2\theta_1 = 0$. We therefore have

$$\theta_1 = -K\left[\frac{1}{4}(r/R)^2 - \frac{1}{16}(r/R)^4 \right.$$

$$\left. + A_0 + \sum_{n=1}^{\infty} A_n e^{-n\alpha}\cos n\beta\right] \qquad (30)$$

and

$$\theta_2 = -K\left[B_0\alpha + \sum_{n=1}^{\infty} B_n \sinh n\alpha \cos n\beta\right]. \qquad (31)$$

The boundary conditions (26) and (29), are already satisfied. Upon satisfying (27) and (28) we obtain

$$A_0 = -\left(\frac{1}{4}\frac{k_1}{k_2}\alpha_0 + \frac{3}{16}\right) \qquad (32)$$

$$A_n = -\frac{(-1)^n \sinh n\alpha_0}{2n[\sinh n\alpha_0 + (k_1/k_2)\cosh n\alpha_0]},$$

$$n = 1, 2, \ldots \qquad (33)$$

$$B_0 = -\frac{1}{4}(k_1/k_2) \qquad (34)$$

and

$$B_n = -\frac{(-1)^n e^{-n\alpha_0}}{2n[\sinh n\alpha_0 + (k_1/k_2)\cosh n\alpha_0]},$$

$$n = 1, 2, \ldots \qquad (35)$$

In order to obtain an expression for the shape factor, we must calculate the fluid bulk temperature, θ_b. This is given by

$$\theta_b = \frac{2}{\pi R^2} \int\int \theta_1(\alpha, \beta)[1 - (r/R)^2]\,dA \qquad (36)$$

where the double integration is carried out over the

cross-sectional area of the pipe. By the representation of (r/R) in the (α, β) coordinates we find that

$$\theta_b = K\frac{11}{96} + \frac{1}{4}(k_1/k_2)\alpha_0 - \frac{4}{\pi}\sum_{n=1}^{\infty}\int_{-\pi}^{\pi}\int_{\alpha_0}^{\infty}$$

$$\times A_n e^{-n\alpha}\left[\frac{\sinh^3\alpha_0 \sinh(\alpha - \alpha_0)\cos n\beta}{(\cosh\alpha + \cos\beta)^3}\right]d\alpha d\beta. \qquad (37)$$

After tedious evaluation of the above double integral, we obtain

$$\theta_b = K\left[\frac{11}{96} + \frac{1}{4}(k_1/k_2)\alpha_0 - \sum_{n=1}^{\infty} A_n e^{-2n\alpha_0}\right]. \qquad (38)$$

The heat flow per unit length of the pipe is given by an expression comparable to equation (14). The shape factor [defined in equation (19)] is

$$S = \left[\frac{11}{24}(k_1/k_2) + \alpha_0 + 2\sum_{n=1}^{\infty}\right.$$

$$\left.\times \frac{(k_2/k_1)e^{-2n\alpha_0}}{n[\coth n\alpha_0 + (k_2/k_1)]}\right]^{-1}. \qquad (39)$$

The first term in equation (39) is identical to the classical result for a pipe with uniform heat flux at its surface [2]. The second term is identical to the thermal resistance for an isothermal buried pipe, and the third one can be viewed as a correction term whose magnitude decreases with increasing α_0.

5. DISCUSSION

In this section we compare calculations obtained by using the two models presented in the previous sections. Since the description of the laminar temperature field inside the pipe will assist us in better understanding the similarities and the differences between the two models, we start by introducing the vertical temperature profile inside the pipe for various burial depths (D/R) and various thermal conductivity ratios (k_2/k_1). These temperature distributions are shown in Figs. 4 and 5 respectively. The abscissa is the normalized temperature θ_1/θ_b, and the ordinate is the radial location with respect to the pipe center. These temperature profiles correspond to the laminar case, and their asymmetric structure is apparent. The maximum temperature always occurs below the center-line of the pipe; but as the burial depth increases, the location of the maximum temperature migrates towards the pipe center (Fig. 4). Consequently, the temperature at the bottom of the pipe decreases with increasing burial depth. The dependence of the temperature profile on the thermal conductivity ratio k_2/k_1 is shown in Fig. 5. We note that for high k_2/k_1 ratios, the relatively high thermal conductivity of the medium tends to equalize the temperature distribution on the pipe surface and forces the temperature profile inside the pipe to be almost symmetric. Hence, the location of the temperature apex migrates towards the pipe center with increasing k_2/k_1. For low k_2/k_1 ratios, the relatively high conductivity of the fluid tends to
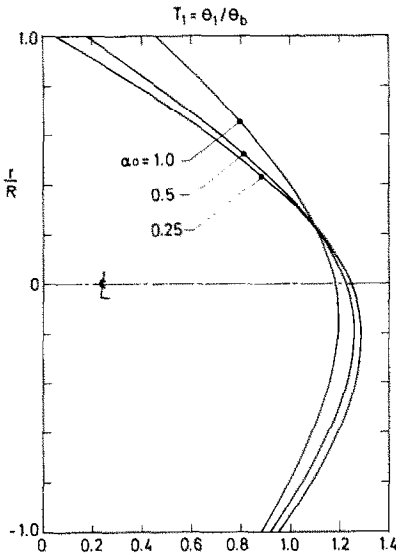
FIG. 4. The normalized temperature profile (θ/θ_b) in the pipe is shown for various burial depths $\alpha_0 = 0.25, 0.5,$ and $1.$ $(D/R = 1.031, 1.128$ and $1.543)$. The medium–fluid thermal conductivity ratio is $k_2/k_1 = 1$.

flatten the temperature profile and to decrease the asymmetry.

Note that the physical properties in the laminar and turbulent models are described by the fluid thermal conductivity ratio (k_2/k_1) and by the Biot (Bi) number, respectively. To facilitate comparison we assign for h in the latter case the classical value

$$Nu = \frac{hR}{k_1} = \frac{24}{11},$$

which is the Nusselt number for pipe flow with uniform heat flux at the surface [2]. Using this value, we obtain
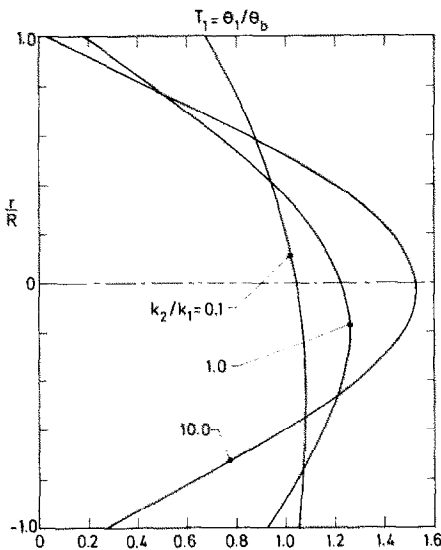

FIG. 5. The normalized temperature profile (θ_1/θ_b) in a pipe buried at depth $\alpha_0 = 0.5$ $(D/R = 1.128)$ is shown for various medium–fluid thermal conductivity ratios $k_2/k_1 = 0.1, 1, 10$.

a relationship between the two parameters, (Bi) and (k_2/k_1), in the form

$$Bi = \frac{hR}{k_2} = \frac{24}{11}\frac{k_1}{k_2}. \tag{40}$$

Hence, when comparing the two cases we shall use the corresponding values satisfying the above relationship.

The temperature distribution around the pipe surface is shown in Figs. 6 and 7 respectively as a function of the burial depth and the thermal conductivity ratio (k_2/k_1). The ordinate is the normalized temperature θ/θ_b, and the abscissa is β. The dashed and solid lines represent the turbulent and the laminar models respectively. The qualitative behavior in both cases is similar. Since in the turbulent model there are temperature extrema in the pipe, the peak temperature at the pipe bottom tends to be lower than in the case of the laminar model. A marked difference between these two models is that the ratio θ/θ_b at the pipe bottom rises with increasing burial depth for the turbulent model while it declines for the laminar one (Fig. 6). The dependence of the temperature profile on the thermal conductivity ratio (k_2/k_1) is shown in Fig. 7. The results for the laminar and turbulent cases almost coincide for high k_2/k_1 ratios. This may have been expected since the relatively high thermal conductivity of the fluid tends to equalize the temperature inside the pipe (Fig. 5).

Finally, in Fig. 8 we present the shape factor (S) as a function of the burial depth (α_0) for various values of k_2/k_1 (or Bi). The dashed and solid lines represent the turbulent and laminar cases respectively. The ordinate is the ratio of the actual shape factor S normalized by the shape factor of an isothermal pipe $(1/\alpha_0)$. The abscissa is the burial depth, shown in terms of α_0 and D/R at the bottom and top respectively. The general characteristics of Fig. 8 are in agreement with the previous figures. For high values of k_2/k_1, the laminar model approaches symmetry and the heat transfer coefficient on the pipe surface is almost uniform; thus the results of both models coincide. For low values of k_2/k_1 and for large values of α_0, we expect to approach a situation of an isothermal pipe and again both
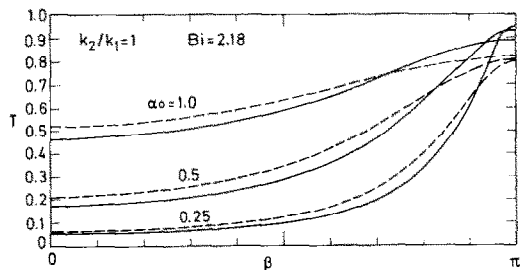

FIG. 6. The temperature distribution around the pipe surface is shown for pipes buried at various depths $\alpha_0 = 0.25, 0.5$ and $1.$ $(D/R = 1.031, 1.128$ and $1.543)$. The medium–fluid conductivity ratio is $k_2/k_1 = 1$, and the corresponding Biot number is $Bi = 2.18$. The dashed and solid lines correspond to the turbulent and laminar cases, respectively.
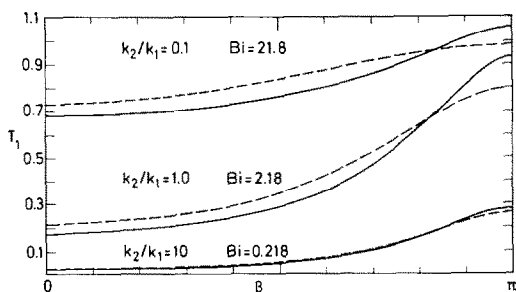
FIG. 7. The temperature distribution around the pipe surface for a pipe burial at depth $\alpha_0 = 0.5\,(D/R = 1.120)$ is shown for various medium–fluid thermal conductivity ratios. The dashed and solid lines correspond to the turbulent and laminar cases respectively.
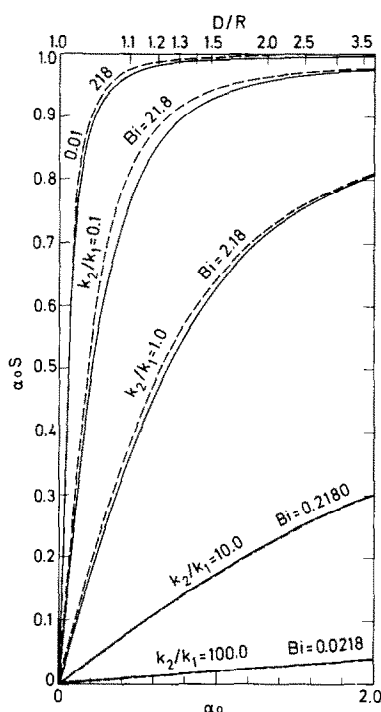

FIG. 8. The shape factor is shown as a function of the burial depth (α_0) for various fluid–medium thermal conductivity ratios. The dashed and solid lines correspond to the turbulent and laminar cases respectively.

models give similar results. It is interesting to note that the deviation between the two models is always smaller than 10%. Consequently, the simple expression (22) can be used even for the laminar–asymmetric case with relatively small error.

6. CONCLUSION

We have derived expressions for the temperature distribution and the shape factor for turbulent and laminar flow in a buried pipe. In the former case, we assume a uniform heat transfer coefficient at the pipe

surface, and we find that the expression for the shape factor

$$S = \frac{Bi}{(1 + Bi^2\,\alpha_0^2 + 2\,Bi\,\alpha_0\coth\alpha_0)^{1/2}}$$

is accurate within 2%. In the laminar case, although the temperature profile in the pipe is asymmetric, the above expression provides results which are accurate within 10%.

REFERENCES

1. E. Hahne and U. Grigull, A shape factor scheme for point source configurations. Int. J. Heat Mass Transfer 17, 267–273 (1974).
2. E. R. G. Eckert and R. M. Drake, Analysis of Heat and Mass Transfer, pp. 98 and 340. McGraw-Hill (1972).
3. M. M. Yovanovich, Advanced Heat Conduction, to be published.
4. N. N. Lebedev, I. P. Skalskaya and Y. S. Uflyand, Worked Problems in Applied Mathematics. pp. 212–213. Dover (1979).
5. R. Thiyagarajan and M. M. Yovanovich, Thermal resistance of a buried cylinder with constant flux boundary condition, Trans. Am. Soc. Mech. Engrs. Series C, J. Heat Transfer 96, 249–250 (1974).
6. I. A. Ioffe, A problem of transient heat conduction in a semi-bounded body with an internal heat source. Inzh. Fiz. Zh. 23, 351–355 (1972). English translation: J. Engng Phys. 23, 1051–1054 (1972)].
7. W. W. Martin and S. S. Sadhal, Bounds on transient temperature distribution due to a buried cylindrical heat source, Int. J. Heat Mass Transfer 21, 783–789 (1978).
8. M. M. Yovanovich, personal communication (1981).

APPENDIX

The purpose of this Appendix is to show that the approximate shape factor, equation (22), is a lower bound of the exact shape factor, equation (21).

Yovanovich [8] suggests a method of obtaining a lower and upper bound for the shape factor (S). The lower bound is obtained by considering a flux tube bounded by two constant β surfaces (Fig. 1), say, β and $\beta + d\beta$. In effect, the surfaces β and $\beta + d\beta$ can be viewed as insulated partitions. Consequently, no heat flow is allowed along constant α lines. The thermal resistance of such a section will be the sum of the film resistance inside the pipe and the conductive resistance inside the flux tube. The shape factor can be written as the inverse of the resistance

$$dS = \frac{1}{2\pi k_2}\left\{\frac{1}{hR[g(\alpha_0,\,\beta)]^{1/2}\,d\beta}\right.$$

$$\left. + \int_0^{\alpha_0}\frac{[g(\alpha,\,\beta)]^{1/2}\,d\alpha}{k_2[g(\alpha,\,\beta)]^{1/2}\,d\beta}\right\}^{-1} \quad (A1)$$

Integration over β yields the lower bound for the shape factor

$$S_t = 2\int_{\beta=0}^{\beta=\pi} dS. \quad (A2)$$

The expression we obtain here is identical to our approximate shape factor, equation (22). This however, should not

Table A1. Comparison between the exact shape factor (S), the approximate shape factor (S_1) and the upper bound (S_u)

α_0	D/R	$Bi = 0.1$			$Bi = 1$			$Bi = 10$			$Bi = 100.0$		
		S_1	S	S_u	S_1	S	S_u	S_1	S	S_u	S_1	S	S_u
0.1	1.005	0.0913	0.0919	0.0990	0.576	0.585	0.909	2.129	2.137	5.0	5.757	5.760	9.091
0.2	1.020	0.0912	0.0918	0.0980	0.571	0.580	0.833	1.989	1.997	3.333	4.070	4.071	4.762
0.3	1.045	0.0910	0.0917	0.0971	0.563	0.572	0.769	1.808	1.814	2.5	3.006	3.006	3.226
0.5	1.128	0.0906	0.0912	0.0952	0.541	0.549	0.667	1.449	1.452	1.667	1.918	1.918	1.961
1.0	1.543	0.0886	0.0892	0.0909	0.465	0.470	0.5	0.886	0.887	0.909	0.987	0.987	0.990
2.0	3.762	0.0826	0.0831	0.0833	0.331	0.331	0.333	0.475	0.475	0.476	0.497	0.497	0.498

be surprising since the expression (22) has been calculated by using the 1-dim. equation, $\dfrac{\partial^2 T}{\partial \alpha^2} = 0$. In this equation we implicitly do not allow heat flow along constant α lines. Hence, our 1-dim. approximation is comparable to the flux tube model, and our approximate shape factor, equation (22), is a lower bound.

Yovanovich [8] also suggests a method of constructing an upper bound to the shape factor. On the assumption that the pipe is isothermal, we obtain the upper bound for the shape factor (S_u)

$$S_u = \frac{Bi}{1 + Bi\alpha_0}. \qquad (A3)$$

This is identical to our approximate shape factor for large α_0 [equation (21a)].

It is interesting to check how close these upper and lower bounds are to the exact solution. We exhibit this information in Table A1 where we present the exact shape factor and the upper and lower bounds for various values of α_0 and the Biot number.

As is evident from the table, the difference between the upper and lower bounds decreases for large values of α_0, small values of Bi and large values of Bi. However, in the range of moderate Biot numbers and small α_0, there is a fairly large gap between the lower and upper bounds. We note also that the exact value is remarkably close to the lower bound. The maximum deviation is well below 2%.

It is difficult to provide a rigorous explanation as to why the lower bound is so close to the exact solution. We note, however, that the temperature distribution associated with the lower bound (19) satisfies the differential equation (1) in an average sense and it also satisfies the boundary condition at the pipe wall, while the temperature distribution associated with the upper bound does not satisfy the same boundary condition. Consequently, the surface temperature associated with the lower bound resembles very closely the exact one as is evident from Fig. 2. On the other hand, the surface temperature associated with the upper bound differs significantly from the exact one. For example, the isothermal surface temperature for $\alpha_0 = 0.25$ and $Bi = 1$ is 0.20. We see that this isotherm (Fig. 2) is much above the exact temperature in the upper section of the pipe. For this reason, the shape factor associated with this isothermal temperature is well above the exact value. On the other hand, the temperature distribution associated with the lower bound is only slightly below the exact temperature distribution in the same region. Consequently, the lower bound is very close to the exact shape factor.

PERTES DE CHALEUR A PARTIR D'UN FLUIDE EN ECOULEMENT DANS UN TUYAU ENTERRE

Résumé—On présente des solutions analytiques pour les pertes de chaleur à partir d'un tuyau enterré. On considère deux cas. Le premier suppose une condition aux limites mixte (convective) avec un coefficient de transfert thermique uniforme à la surface du tube, ce qui est le cas de l'écoulement turbulent. Une expression simple approchée, précise à 2% près est obtenue pour le facteur de forme dans ce cas. Dans le second cas, on considère un écoulement laminaire avec une variation laminaire le long de l'axe du tube. Le couplage du transfert thermique à l'intérieur et à l'extérieur du tube demande la résolution simultanée des équations de l'énergie pour ces deux régions. La géométrie compliquée est prise en compte d'une façon élégante par l'utilisation du système bicylindrique de coordonnées. Les résultats concernent les distributions de température et le facteur de forme dans chaque cas.

WÄRMEVERLUSTE EINES DURCH EIN EINGEGRABENES ROHR STRÖMENDEN FLUIDS

Zusammenfassung—Es werden analytische Lösungen für die Wärmeverluste eines eingegrabenen Rohres angegeben. Zwei Fälle werden betrachtet: Der erste Fall enthält eine gemischte (konvektive) Randbedingung mit einem gleichförmigen Wärmeübergangskoeffizienten an der Rohroberfläche, was für turbulente Strömung zutrifft. Ein einfacher Näherungsausdruck für den Formfaktor dieses Falles wird mit einem größten Fehler von kleiner 2% hergeleitet. Im zweiten Fall wird eine laminare Strömung mit linearer Temperaturänderung entlag der Rohrachse betrachtet. Der gekoppelte Wärmeübertragungsprozeß innerhalb und außerhalb des Rohres efordert die simultane Lösung der Energiegleichungen für diese beiden Gebiete. Die komplizierte Geometrie wird in eleganter Weise mit einem bizylindrischen Koordinatensystem behandelt. Die Ergebnisse enthalten die Temperaturverteilung und den Formfaktor für jeden Fall.

ПОТЕРИ ТЕПЛА ЖИДКОСТЬЮ ПРИ ТЕЧЕНИИ В ЗАГЛУБЛЕННОЙ ТРУБЕ

Аннотация—Представлены аналитические решения для определения потерь тепла заглубленной трубой. Рассмотрены два случая. В первом используется смешанное (конвективное) граничное условие с однородным коэффициентом переноса тепла на поверхности трубы, который имеет место при турбулентном течении. Для форм-фактора выведено простое приближенное выражение, дающее погрешность в пределах 2%. Во втором случае рассматривается ламинарное течение с линейным изменением температуры по оси трубы. Взаимодействие процессов теплопереноса внутри и снаружи трубы требует одновременного решения уравнений энергии для этих двух областей. Для рассмотрения сложной геометрии применяется изящный метод с использованием бицилиндрической системы координат. Получены результаты по распределению температур и форм-факторам для каждого случая.